Journal of Membrane Science 635 (2021) 119543

Contents lists available at ScienceDirect

Journal of Membrane Science

journal homepage: www.elsevier.com/locate/memsci

Performance optimization of diamine cross-linked mixed matrix membrane for high value organic acid recovery

Nadiah Khairul Zaman [a], Rosiah Rohani [a,*], Izzati Izni Yusoff [a], Abdul Wahab Mohammad [a], Abdullah Amru Indera Luthfi [a], Suriani Abu Bakar [b]

[a] Department of Chemical & Process Engineering, Faculty of Engineering and Built Environment, Universiti Kebangsaan Malaysia, 43600, UKM, Bangi, Selangor, Malaysia

[b] Department of Physics, Faculty of Science and Mathematics, Universiti Pendidikan Sultan Idris, Tanjung Malim, 35900, Perak, Malaysia

ARTICLE INFO

Keywords:
Diamine
Polyimide
Crosslinking
Optimization
Modelling
Organic acid

ABSTRACT

A modelling and optimization approach was implemented for the succinate recovery, a high-value organic acid, from concentrated feeds using polyimide (PI)/graphene oxide (GO) mixed matrix membrane (MMM) cross-linked with ethylenediamine (EDA). The effects of parameters, including i) time for crosslinking, ii) time for solvent evaporation, and iii) feed concentration, on succinate rejection and separation factor (SF) were investigated. The optimization of the dominant factors, namely, crosslinking time and succinate concentration, greatly enhanced the succinate rejection and SF, where 73% initial drop in succinate rejection was improved, and a membrane rejection performance of above 80% was sustained, even when the succinate concentration rose to 50 g/L. This improvement was attributed to the formation of covalent bonds and a reduction in the d-spacing of the cross-linked MMM. The optimization study with a desirability of 0.81 also demonstrated the applicability of the model to an actual broth. The optimized membrane prepared at 1.61 h crosslinking time, 30 s evaporation time and 30 g/L succinate concentration demonstrated 86% succinate recovery from the actual broth, 0.15-0.33 SF, and 96% flux recovery ratio. Thus, this optimization study could be a way forward in exploring, simultaneously expanding cross-linked membrane applications especially in product recoveries from concentrated feed(s).

1. Introduction

Bio-succinic acid is a potential high-value organic acid, and it is among the top twelve chemical building blocks derived from renewable resources, which are also known as potential platform chemicals [1]. Its demand has been growing continuously, and presently, it has reached a market size of USD 530.9 million. By 2026, the market for bio-succinate is expected to expand further and is forecasted to be equivalent to a compound annual growth rate (CAGR) of 25.99%, with a market value of USD 675.1 million [2,3]. The significant expansion of the bio-succinic acid market has encouraged intensive development of the production of bio-based succinic acid, which could be of great benefit as it is a biomass that is available in abundance. However, unlike the traditionally-derived succinic acid, bio-succinic acid requires stages of treatment, and separation and purification processes to obtain a high-purity product [4]. Among the current dominant downstream technologies utilized is the precipitation process, which can induce the excessive generation of secondary salts, where further treatment such as thermal cracking is needed, which, without proper handling could cause an overall environmental footprint. The precipitation technique is being practised by Myirant and BASF-Purac JV, the leading developers in the industry [5]. Therefore, the membrane separation process technology has attracted much attention for its application in the recovery of bio-succinic acid as it has energy-saving and environment-friendly features [5,6]. Thus, the overall membrane technology process was enhanced by making improvements to the membrane and the process.

The working of a nanofiltration (NF) membrane is based on the separation principle of electrostatic repulsion (Donnan exclusion) and/or the exclusion of small ions and molecules (steric effect) [7]. The separation performance is significantly influenced by the membrane properties, which are continuously being improved to combat various issues with the membrane such as the trade-off limitation between selectivity and permeability, reduced membrane performance over time, fouling effect, and low membrane rejection and/or selectivity. In the recovery of bio-succinic acid, the main setback that has been identified is the reduced NF membrane rejection and selectivity when dealing with

* Corresponding author.
E-mail address: rosiah@ukm.edu.my (R. Rohani).

https://doi.org/10.1016/j.memsci.2021.119543
Received 23 April 2021; Received in revised form 15 June 2021; Accepted 18 June 2021
Available online 22 June 2021

a concentrated product and/or relatively high concentrations of by-products. In previous studies, reports on high succinic rejection and selectivity performance were found to be only limited to the feed having a succinate concentration of around 10–40 g/L [8,9], with relatively low concentrations of by-products that are more than 8–10 times lower than that of the product [10,11]. However, presently, the production of a higher concentration of bio-succinic acid has been made possible through the utilization of various types of renewable carbon sources and a wide range of metabolic engineered microorganisms. Succinic acid has been produced at various concentrations ranging from as low as 10 g/L up to 68 g/L, with different concentrations of by-products, subject to the conditions of the production process [10]. However, at a higher concentration of the feed solution, the recovery using membrane technology is usually a great challenge due to the complexity of the feed. A concentrated feed can reduce or screen the membrane charge effect, decrease the solute diffusivity from an increased feed viscosity, increase the osmotic pressure, and induce changes to the membrane structure, which can result in a decrease in the membrane rejection performance [12,13].

Therefore, since it was observed that many factors from the process and fabrication conditions could influence the efficiency of the recovery process, optimization was seen as the best approach. Optimization using the response surface method (RSM) can increase the efficiency and shorten the time for determining the influence of individual factors as well as the effects of the interaction of factors, which are hard to achieve with conventional multifactor experiments. In this study, a statistical approach was developed to optimize the performance of the membrane – the fabrication conditions in relation to the ethylenediamine (EDA)-crosslinked polyimide/graphene oxide (PI/GO) mixed matrix membrane (MMM). As far as is known, this is the first proof-of-concept study for validating the approach of tackling the problem of a reduced membrane rejection of succinate when a concentrated feed solution (up to 50 g/L) is utilized. This study was a continuation of the successful application of a PI membrane modified with GO (PI/GO MMM) for sustaining the membrane recovery performance of sodium sulphate (Na_2SO_4) at an elevated concentration of more than 98%, of which, with a neat membrane, a reduction in rejection of 16% was reported in a previous study [14]. With the addition of GO to the PI polymer matrix, the reduction in rejection of Na_2SO_4 at increasing concentrations from 5 to 150 mM (21.3 g/L) was successfully overcome. In the previous study, it was found that the presence of GO altered the properties of the MMM and created enough resistance to prevent the ions from passing through the membrane. Therefore, the membrane was able to sustain its high rejection performance regardless of the filtration feed concentration [15,16].

In relation to this study, as similar charged ions were utilized (succinate and sulphate ions), the PI/GO MMM was expected to give a similar performance regarding the recovery of succinate from a concentrated feed solution. However, an additional crosslinking process using EDA was introduced in this study to ensure that the membrane performed well in an actual fermentation broth and in long-term applications. EDA is a very hydrophilic compound and it possesses the shortest chains among the diamine groups. It is believed that the former property can enhance the permeability of the membrane, while the latter can minimize the crosslinking time as it can be easily absorbed into the membrane matrix for the crosslinking reaction to occur [17]. To date, chemical cross-linking of membranes has been widely adopted to improve the properties and performance of membranes. This includes reducing the plasticization of the membrane, which could result in the loss of separation performance and improved membrane stability by preventing excessive swelling [18–20]. In other studies, the crosslinking process was also implemented to tune the structure of the membrane and to improve the tightness of the nanofiltration membrane for a high rejection performance [21–23].

The optimization was conducted by studying three key input factors governing the optimum values and the effects of interaction on the performance of a membrane. The key factors (independent variables) that were investigated included the time for membrane crosslinking, the time for the solvent to evaporate from the membrane phase prior to the phase inversion process, and the concentration of the feed solution. The use of fabrication conditions instead of membrane properties as inputs in the optimization study is due to its importance in identifying the most influential parameters so that it could reduce future workload for the optimization. However, the applicability of the identified conditions could be limited given the specificity of the substrates utilized. Meanwhile, the responses included the succinate rejection and the separation factors (SFs) of the succinate over the by-products (formate and acetate). The statistical evaluation was carried out using RSM, while a Box-Behnken experimental design was used to provide data for the modelling. Other analyses, such as membrane characterizations to evaluate membrane properties and other statistical analyses of variance (ANOVA) and Pareto, were also carried out to further assess the adequacy of the resulting models statistically, the significance of each term in these models, and to signify the relative effects of the first order, quadratic, and interaction terms on the responses, respectively. The validation of the optimum conditions achieved was also carried out using an actual fermentation broth with variables selected according to previous studies [8,24–26].

2. Methodology

2.1. Membrane fabrication and crosslinking

The details of the utilized materials and the fabrication of the PI/GO MMM can be referred to in a previous study [14]. In brief, the materials used included PI P84 (Good Fellow, Cambridge Ltd), synthesized GO and N-methyl-2-pyrrolidinone (NMP, Merck Millipore) for the MMM fabrication. Other solvents utilized were sulphuric acid (H_2SO_4, R&M Chemical), phosphoric acid (H_3PO_4, R&M Chemical), hydrogen peroxide (H_2O_2, R&M Chemical) and potassium permanganate ($KMnO_4$, Sigma-Aldrich). Meanwhile, for the post-synthesis (POST) crosslinking, ethylene diamine (EDA, R&M Chemical) and methanol (Merck Millipore) were used.

For the preparation of the membrane, 0.9 wt% of PI/GO MMM was selected due to its best performance, as reported in a previous study [14]. A doped solution containing PI, GO and NMP was prepared and stirred until it was homogeneous. The solution was then deposited on a glass slide and cast using an automatic casting knife (Elcometer 4340) at a constant thickness of 150 μm. In this study, the evaporation of the solvent from the membrane phase prior to the phase inversion process was varied at 30, 45 and 60 s. The preparation of the polymer films was then finalized by dipping the glass into ultrapure (UP) water. The detailed preparation of the membrane can be found in a previous study [14]. From the polymer films, crosslinked MMMs were prepared via the POST crosslinking technique adapted from a previous study [27]. The MMM was immersed in a methanol solution containing 2.5 wt% of EDA, and was then rinsed with methanol to remove the remaining crosslinker. The crosslinking time was varied at 0, 1 and 2 h.

2.2. Membrane characterizations

The crosslinked MMM was evaluated in terms of its physical, chemical, and crystalline properties. A Nicolet 6700 Fourier transform infrared spectrometer (FT-IR, Thermo Fischer Scientific) was utilized to monitor the chemical changes in the MMM before and after the crosslinking. A D8 Advanced X-ray diffraction (XRD, Bruker AXS) technique was utilized to characterize the non- and crosslinked PI/GO MMMs. Meanwhile, the contact angle was analysed by means of a drop shape analysis (DSA, Kruss GmbH). The conditions for all the analyses can be found in a previous study [14].

The gel content of the cross-linked membrane was also analysed by gravimetric analysis, where the membrane was initially dried, weighed

(W_a) and immersed in DMF for two weeks. The membrane was then dried again, and the final weight was measured (W_c). The gel content of the cross-linked membrane was calculated using Eq. (1). Further confirmation of the stability of the cross-linked membrane was visually evaluated by immersing the membrane in NMP for another two weeks.

$$Gel\ content = \frac{W_c}{W_a} x\ 100 \quad (1)$$

The swelling property of the membrane was also evaluated by gravimetric analysis, where the degree of membrane swelling was determined from the difference in the weight of the membrane before (indicated by m_0) and after (indicated by m_1) the crosslinking process. For the membrane swelling process, the membrane was soaked in 30 g/L of succinate solution for 1 h, and the process was repeated until equilibrium was achieved. A filter paper was used to absorb the excess solution on the surface of the membrane. The swelling ratio, M_g was calculated using Eq. (2):

$$M_g = \frac{m_1 - m_0}{m_0} \quad (2)$$

2.3. Synthetic model solution, actual fermentation broth and analysis

For a statistical analysis, model solutions were used throughout the study. The mixture solutions, consisting of succinate as the product and formate and acetate as the by-products, were prepared initially by weighing every salt using a weighing balance. A 1-L volumetric flask was used to dissolve the salts using deionized water (DI). The concentrations of the mixture were set at 10, 30 and 50 g/L of succinate, with the by-products set at a consistent ratio of 1:2 (by-product: product). All the samples were analysed using high-performance liquid chromatography (HPLC, UltiMate 3000 LC system, Dionex), with conditions based on a previous study [14].

The developed model was also validated using an actual fermentation broth received from the Biohydrogen Research Group, Department of Chemical and Process Engineering, Universiti Kebangsaan Malaysia, which was a research team that was working together in this study. Prior to the membrane separation process, the broth was initially centrifuged (Eppendorf Centrifuge 5804) for 20 min at 8000 rpm for the cell biomass and macromolecule separation, followed by pre-treatment using activated carbon adsorption to remove any remaining glucose residue and colour impurities. The pre-treated sample was then analysed using HPLC to determine its properties. The organic acid product was mainly present in its salt form rather than as a free acid due to the nearly neutral pH condition of the broth (6.8). Thus, the term succinate was used instead of succinic acid. Table 1 presents the properties and concentrations of the main components that were present in the broth after the pre-treatment.

2.4. Experimental design and statistical analysis

A statistical evaluation of the modified PI/GO MMM using the EDA crosslinker was carried out using Design-Expert 6 software (Stat-Ease Inc, USA). A Box-Behnken design was established to perform 17 runs with three input factors. It was a second-order technique class based on a three-level factorial design for three factors or more, where the design arrangement was that of a cube or three interlocking 22 factorial designs with a central point. The input factors were selected based on their significant effect on the succinate recovery, including: (i) crosslinking times of 0, 1 and 2 h, (ii) times for the evaporation of the solvent from the membrane phase prior to the phase inversion at 0, 30 and 60 s, and (iii) succinate concentrations of 10, 30 and 50 g/L in the mixture. For the mixture concentration, the ratio of the succinate to formate and acetate was kept constant at 5:2. Table 2 shows the selected factors with 3 coded levels (−1, 0, 1).

From the input factors, three responses were evaluated, which included the succinate rejection, succinate/formate SF, and succinate/acetate SF. The performance of the membrane was measured using a dead-end filtration cell (Sterlitech HP4750, USA) at process conditions of a stirring speed of 800 rpm, operating pressure of 30 bar, temperature of 25 °C, and feed volume of 100 mL, according to the previous study [7]. The membrane, with an area of 0.00146 m^2 (Sterlitech USA), was clamped inside the filtration unit and pressurized at 35 bar until a steady flow was achieved. The experimental set-up is illustrated in Fig. 1. The permeation of the membrane was then calculated using Eq. (3) and its rejection and SF were calculated using Eq. (4) and Eq. (5), respectively:

$$J = \frac{nV}{t.A} \quad (3)$$

where J represents the flux ($L/m^2.h$), V represents the volume (L), and t and A represent the time (min) and effective area of the membrane (m^2), respectively.

$$R\ (\%) = \left[1 - \frac{C_p}{C_f}\right] x\ \ 100 \quad (4)$$

where R is the percentage of rejection (%), C_P is the permeate concentration (g/L), and C_f is the feed concentration (g/L).

$$SF = \frac{1 - R_{suc}}{1 - R_{by-product}} \quad (5)$$

where R_{suc} is the rejection of the succinate, and $R_{by\text{-}product}$ is the rejection of the by-product.

To statistically evaluate the performance of the membrane on the succinate recovery, a mathematical model generated by RSM was utilized, and the model was presented as a second-degree polynomial. The model evaluated the consistency between the experimental and predicted responses, where the evaluation of the model fit was mandatory. Each measured response from the experiment was correlated with the model presented in Eq. (6):

$$Y_i = b_0 + \sum_{i=1}^{n} b_i x_i + \sum_{i=1}^{n} b_{ii} x_i^2 + \sum_{i=1}^{n-1} \sum_{j=i+1}^{n} b_{ij} x_i x_j \quad (6)$$

where Y_i is the predicted response factor, b_0 is the intercept term, b_i is the linear coefficient, b_{ii} is the 2nd order polynomial coefficient, b_{ij} is the interaction term, and x_i and x_j are the coded values for the variables.

Apart from that, the validity of the model was also determined from the coefficient of determination (R^2) and the analysis of variance (ANOVA) generated by the mathematical models. The ANOVA provided an understanding of the interaction between the modified membrane and the process parameters, and the performance of the membrane regarding the succinate. Meanwhile, a Pareto analysis was utilized to determine the most significant inputs on the responses. It arranged the inputs that mattered in order of importance. The Pareto analysis was

Table 1
Main composition of fermentation broth (pH = 6.8).

Component	Molecular Formula	Molecular Weight (g/mol)	Concentration (g/L)
Succinate	$C_4H_6O_4^{2-}$	116.07	30.0
Formate	CHO_2^-	45.02	4.9
Acetate	$C_2H_3O_2^-$	59.04	8.0

Table 2
Factors for Box-Behnken design of succinate recovery from model solution using POST-treated PI/GO MMM.

	Factors	Levels		
		−1	0	1
A	Post-treatment time (h)	0	1	2
B	Evaporation time (s)	0	30	60
C	Succinate feed concentration in a mixture (g/L)	10	30	50

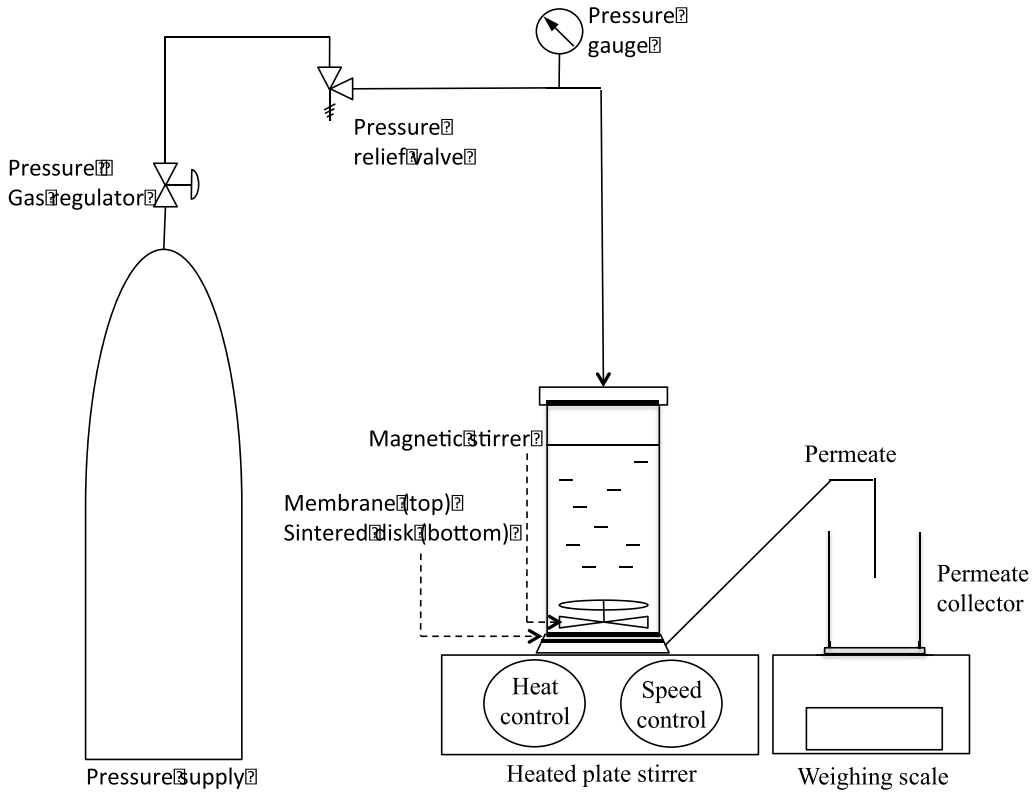

Fig. 1. Illustration of dead-end filtration cell set-up (HP4750-stirred cell).

carried out by initially calculating the factor percentage effect (P_i) of each term using Eq. (7):

$$P_i = \left(\frac{\beta_i^2}{\sum_{i=1}^{n}\beta_i^2}\right) x \ \ 100 \tag{7}$$

where β_i is the regression coefficient of the model terms.

Next, the adequacy of the proposed model was also validated. In the final step of the RSM study, the optimum level to achieve a high succinate rejection and selectivity from the mixture solution containing succinate, formate and acetate was determined using a numerical optimization tool embedded in the Design Expert software. The numerical optimization works by probing the design space via the fitted regression model. Then, the combinations of variables that defined the objective of this study were identified using the overall desirability function that had to be maximized. It was expected that the higher the desirability function (D = 1.000), the higher would be the accuracy of the model [28]. In this work, the input variables were given by the specific range values for the crosslinking time, membrane evaporation time and succinate concentration in the feed. The experimental runs were carried out using the predicted optimal input conditions.

The estimated errors between the predicted and experimental values of the succinate rejection and SFs of succinate/formate and succinate/acetate were then calculated using Eq. (8).

$$\text{Error} \ \ (\%) = \frac{(\text{Experimental} \ \ \text{Value} - \text{Predicted} \ \ \text{Value})}{\text{Experimental} \ \ \text{Value}} \tag{8}$$

2.5. Diafiltration with actual fermentation broth

Diafiltration was carried out using 100 ml of the feed solution by means of dead-end filtration cells similar to the NF membrane setup discussed in Section 2.5. A filtration pressure of 30 bar was used, and the filtration process was maintained until a volume concentration factor (VCF) of 1.7 was achieved, representing approximately 80 ml of permeate recovered. Samples of the permeate were taken every 5 min throughout the experiments. After the first cycle of the diafiltration, pressure was released, the retentate volume and weight were recorded, and a sample was taken for analysis using HPLC. A 2nd cycle of filtration was then continued by adding distilled water to the remaining retentate; the feed was kept constant at 100 ml. The diafiltration was repeated for three cycles for a total period of about 300 min. The fouling property of the MMM was also calculated using Eq. (9), which represents the irreversible fouling (R_{ir}), and Eq. (10), which represents the flux recovery ratio (FRR), where the data was collected after the membrane had been subjected to pure water flux permeation at 30 bar for 150 min;

$$R_{ir} = \left(\frac{J_w - J_{wp}}{J_w}\right) x \ 100 \tag{9}$$

$$FRR \ (\%) = \left(\frac{J_{wp}}{J_w}\right) \tag{10}$$

3. Results and discussion

3.1. Characterization of crosslinked membrane

The crosslinking of the PI/GO MMM with EDA was evaluated using FT-IR. Fig. 2 shows the FT-IR spectra of the membrane crosslinked at 0 and 2 h and recorded at wavenumbers ranging from 500 to 4000 cm^{-1}. Overall, Fig. 2 demonstrated that the crosslinking of PI/GO MMM with EDA was successful. This was indicated by the changes in the intensity of five significant peaks, comprised of the peaks from the imide (signified by the grey box) and amine (signified by the green box) bands. From Fig. 2, it can be seen that the MMM that was crosslinked at 0 h exhibited three significant imide absorption peaks at 1335 cm^{-1} (C–N stretching), 1721 cm^{-1} (C═O symmetric stretching) and 1779 cm^{-1} (C═O asymmetric stretching) (signified by the grey boxes), and amine bands at

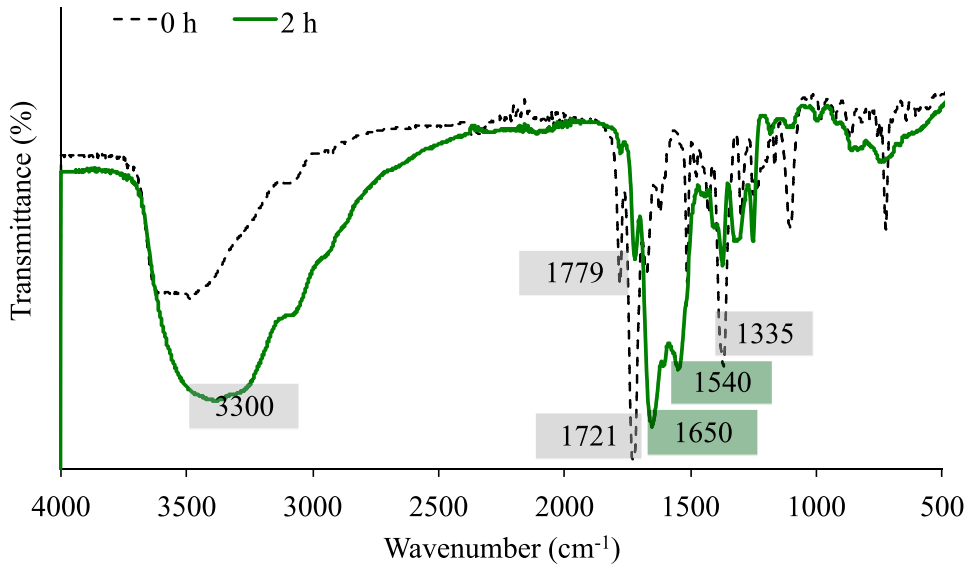

Fig. 2. FTIR of PI/GO MMM at crosslinking times of 0 and 2 h (conditions of membrane; 20 wt% of PI, 0.9 wt% of GO at crosslinking time of 2 h for evaporation time of 30 s).

1540 cm^{-1} (C–N stretching) and 1650 cm^{-1} (N–H bending) (signified by the green boxes), which are the typical bands for PI [17]. As the MMM was subjected to crosslinking, the peak intensity of the imide group was reduced (signified by the grey boxes), and was replaced by increasing intensity of the amine absorption peaks (signified by the green boxes) [29]. The increase in the intensity of the amine peaks and the reduction in the peaks of the imide group indicated that the crosslinking of the membrane with EDA had been successful [29]. The presence of high hydrophilic amine groups in the chemical structure of the PI/GO MMM could have improved the overall hydrophilicity of the membrane, and hence, the permeability of the membrane, which was further confirmed by the contact angle analysis, as discussed in the following paragraph. Amine is well known for its highly water-soluble polar compounds ($-C(=O)NH_2$), which could have helped to increase the hydrophilicity of the membrane [30,31].

Moreover, based on the FT-IR spectra of the cross-linked MMM, most of the covalent bonding was seen to have occurred between the PI chains, based on the significant replacement of the imide by the amine groups and the increasing peak at 3300 cm^{-1}, which indicated the presence of intact O–H stretching on the GO basal plane and additional N–H stretching from the EDA. However, there might have also been a minimum reaction between the EDA with the GO. This is because upon cross-linking with EDA, it was observed that there was a reduction in the 1080 cm^{-1} peak in the PI/GO MMM, which corresponded with the C–O stretching vibrations from the C–O–C group. It was reported in a previous study that EDA can react with carboxylic groups in two ways. It either completely removes the hydroxyl and epoxide moieties, or a reaction can occur without affecting the oxygen in the carboxylic groups [32]. Thus, in relation to this study, as both a reduction and enlargement at the 1080 and 3300 cm^{-1} peaks, respectively were observed, it is believed that the EDA may have reacted with the GO only to a certain extent. According to Mwangi et al. (2012), if the GO reacts completely with the EDA to form covalent bonds, the hydroxyl peak of the GO at around 3000–3500 cm^{-1} in the FT-IR spectrum will be reduced due to the formation of CN-covalent bonds from the condensation reaction process [33]. This result was also in accordance with a previous study, where the blending of GO with the PI polymer was reported to create only hydrogen bonding interactions [14]. The minimum reaction of EDA with GO could ensure minimum to no leaching of GO from the membrane and, at the same time, the unaffected GO functional groups could benefit the overall separation process, sustaining the high membrane rejection performance. Fig. 3 illustrates the formation of covalent bonds with PI and GO. Overall, it is believed that the formation of covalent bonds can improve the performance of the membrane in a concentrated solution by reducing swelling and imposing more resistance for the solute to pass through the membrane, which will be discussed in the following paragraph.

The chemical structure of the MMM crosslinked with EDA was also evaluated using XRD diffraction patterns, which provided information on the intermolecular ordering and in-plane orientation of PI [34]. This is important as the chemical structure of the membrane, such as the d-spacing, could also influence the succinate rejection of the membrane from the concentrated feed solution. Fig. 4 demonstrates that the non-crosslinked MMM had two diffraction peaks. The peak with a d-spacing of 0.48 nm signified the order of the inter-chain packing between the dianhydride and diamine groups. Meanwhile, the other diffraction peak with a d-spacing of 0.36 nm signified the π–π interaction between the neighbouring aromatic rings in the PI structure. The two featured diffraction peaks were also reported in previous studies, indicating the semi-crystalline structure of a neat and modified PI membrane [35,36]. At a crosslinking time of 2 h, it could be seen that the 2θ value of the membrane had shifted to the right, indicating a reduced d-spacing, according to Bragg's Law. The new d-spacings were recorded at 0.40 and 0.34 nm, respectively. However, it is important to note that the d-spacing representing the interaction distance in the chemical structure of PI concerning dianhydrides and diamines could not be used to determine the true inter-chain distance but only to indicate the availability of a free volume for the small molecules to penetrate [31]. Thus, from the results, the crosslinking process that may have occurred between the polymer chains resulted in a tightening of the chains, thus increasing the rigidity of the membrane, reducing the inter-segmental mobility and d-spacing, and enabling the membrane to allow only small molecules to penetrate through it. This could have consequently influenced the rejection performance of the membrane, which will be discussed later in Section 3.3. A similar phenomenon was also observed in previous studies [37–39]. The FT-IR and XRD results were also further supported by the swelling ratio of the membrane in the succinate solution. The swelling ratio of the membrane at a crosslinking time of 2 h was calculated using Eq. (2). It was found that the swelling of the membrane was reduced by around 26, 46 and 41% for the membrane at evaporation times of 30, 45 and 60 s, respectively. It is believed that the reduction in the swelling of the membrane could have improved the

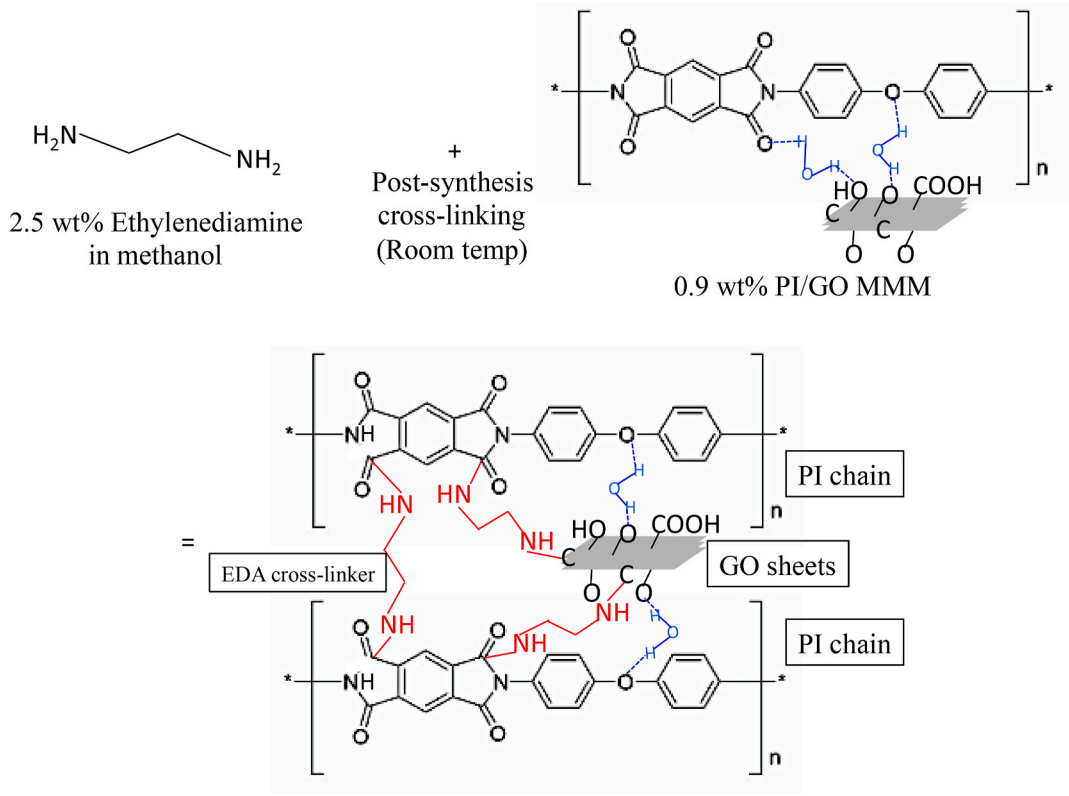

Fig. 3. Proposed schematic formation of covalent bonds between EDA and PI/GO MMM from the crosslinking process.

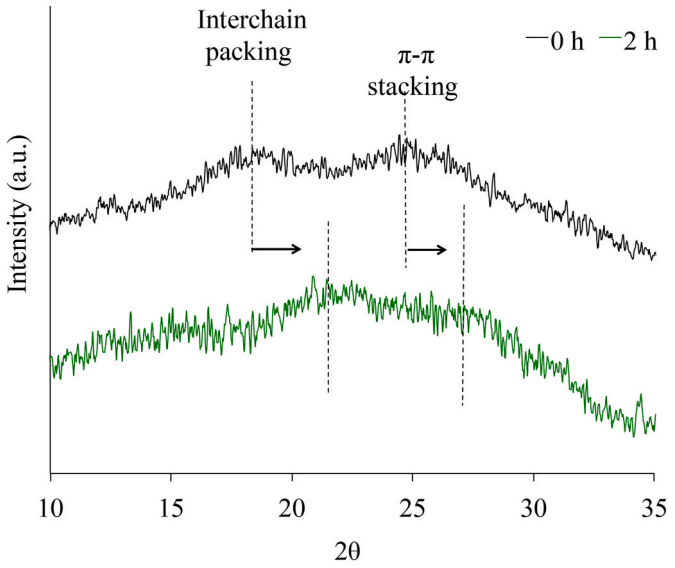

Fig. 4. XRD characterization of PI/GO MMM at crosslinking times of 0 and 2 h (conditions of membrane; 20 wt% of PI, 0.9 wt% of GO at a crosslinking time of 2 h for an evaporation time of 30 s).

rejection performance of the membrane due to the restricted movement in the polymer chains to accommodate big-sized ions, which the relation with membrane performance will be discussed in a later section.

A comparison was also made of the contact angles of the neat PI and the crosslinked and non-crosslinked MMM, and the results are presented in Table 3. According to Table 3, the contact angle of the membrane was reduced with every modification to the PI neat membrane. The contact angle was reduced from 75° to 68° and finally, to 63° for the neat PI, the GO-incorporated PI MMM, and finally the crosslinked MMM, respectively. Such a significant rise in the hydrophilicity of the cross-linked MMM is believed to have been due to the replacement of the functional imide group by the amide group in the PI MMM, which was contributed by the presence of the EDA crosslinker and the properties of the unaffected GO, as discussed in the previous paragraph. The result was also confirmed by FT-IR spectra, as presented in Fig. 2. Finally, the stability of the cross-linked MMM was also evaluated by immersing the membrane in DMF for two weeks. The gel content was calculated using Eq. (1) and the value was successfully obtained at above 90% (refer to Table 3). This result indicated that the membrane has a high stability in a common solvent such as DMF and NMP, thus further confirming the successful crosslinking process, as illustrated in Fig. 3.

3.2. Model fitting and ANOVA analysis

The three final model predictions, as presented in Equations (11)–(13) along with Table 4, were developed using a Box-Behnken design, which later summarized the actual and final model prediction responses with respect to the input variables. The actual and predicted responses were obtained from the experimental runs and mathematical models, respectively (refer to Equations (11)–(13)). From the final model predictions, the consistencies between the experimental and predicted responses were investigated, and the effects of the input factors (A, B and C) on the responses (Y1, Y2 and Y3) were evaluated. The responses from every run showed that the actual responses from the experimental runs were in good agreement with the predicted responses obtained from the mathematical models proposed by an RSM (refer to Table 4).

Table 4 shows that a high accuracy was obtained for the experimental responses compared to the predicted responses, thereby validating the designed model equations. The final model predictions with a constant value, three linear and three quadratic factors, and three interaction terms of input factors are shown as follows:

Table 3
Properties of PI, PI/GO MMM and EDA-crosslinked MMM.

Type of Membrane	Contact Angle (°)	d-spacing (nm)		Swelling in 30 g/L succinate solution		Stability after two weeks soaking in DMF (gel content)
		Inter-chain packing order	π–π interaction	*Evaporation time (s)*	Swelling reduction *(%)*	
PI	75	0.53	0.38	–		Total dissolution
PI/GO MMM	68	0.48	0.36	–		Total dissolution
EDA-crosslinked PI/GO MMM	63	0.40	0.34	*30s*	26	>90%
				45s[a]	46	
				60s[b]	41	

*All membranes were fabricated using 20 wt% of PI and 0.9 wt% of GO at a crosslinking time of 2 h for an evaporation time of 30 s, except for [a, b].

Table 4
Box-Behnken experimental design table of three variables; (A) crosslinking time, (B) membrane evaporation time, and (C) succinate concentration in the feed with the actual and predicted responses of the succinate rejection (Y_1), SF of succinate/formate (Y_2) and SF of succinate/acetate (Y_3).

Std	A	B	C	$Y_{1Actual}$ (%)	$Y_{1Predicted}$ (%)	$Y_{2Actual}$	$Y_{2Predicted}$	$Y_{3Actual}$	$Y_{3Predicted}$
1	0	30	30	46.41	46.76	0.52	0.53	0.75	0.73
2	2	30	30	77.32	73.66	0.21	0.2	0.29	0.26
3	0	60	30	37.69	41.35	0.64	0.65	0.7	0.73
4	2	60	30	77.47	77.12	0.21	0.2	0.33	0.36
5	0	45	10	92.5	89.06	0.38	0.38	0.47	0.47
6	0	45	10	90.68	91.25	0.11	0.12	0.17	0.17
7	0	45	50	24.76	24.19	0.74	0.73	0.8	0.8
8	2	45	50	81.21	84.65	0.21	0.21	0.26	0.26
9	1	30	10	98.23	101.32	0.03	0.022	0.07	0.094
10	1	60	10	92.07	91.85	0.2	0.19	0.28	0.25
11	1	30	50	56.87	57.09	0.35	0.36	0.38	0.41
12	1	60	50	67.71	64.62	0.29	0.3	0.37	0.35
13	1	45	30	75.4	76.75	0.23	0.24	0.29	0.34
14	1	45	30	79	76.75	0.23	0.24	0.39	0.34
15	1	45	30	75.18	76.75	0.26	0.24	0.36	0.34
16	1	45	30	74.06	76.75	0.25	0.24	0.34	0.34
17	1	45	30	80.1	76.75	0.21	0.24	0.34	0.34

$$Succinate Rejection(\%)(Y_1) = 93.9265 + 10.6195A + 1.51335\ B - 3.34946\ C - 11.729A^2 - 0.02354\ \ B^2 + 0.018171C^2 + 0.14783\ A{*}B + 0.72837A{*}C + 0.0142{*}C \quad (11)$$

$$\frac{\text{Succinate}}{\text{Formate}}(\text{separation factor})(Y_2) = -0.10216 - 0.30275A + 0.00611667B + 0.021513C + 0.15013A^2 + 0.000039444B^2 - 0.0000684375C^2 - 0.002A*B - 0.0033125A*C - 0.000192B{*}C \quad (12)$$

$$\frac{\text{Succinate}}{\text{Acetate}}(\text{separation factor})(Y_3) = 0.14356 - 0.50975A + 0.00088333B + 0.028488C + 0.16175A^2 + 0.0000522222B^2 - 0.0002018755C^2 + 0.0015A*B - 0.003A*C - 0.000183B{*}C \quad (13)$$

where Y_1, Y_2 and Y_3 are the rejection of succinate and SFs of succinate/formate and succinate/acetate, respectively, and A, B and C are the crosslinking time, membrane evaporation time and succinate concentration in the mixture [40].

In addition to the responses presented in Table 4, the validity of the model equations was further analysed using the R^2 of every model equation for the succinate rejection (Eq. (11)), SF of succinate/formate (Eq. (12)), and SF of succinate/acetate (Eq. (13)), as presented in Table 5. It was found that the correlation coefficient values were high at 0.98, 0.99 and 0.98, respectively, which indicated that the model equation predictions were in good agreement with the experimental values [41]. In other words, these coefficient values implied that for the succinate rejection, 98% of the variations for succinate rejection were explained by the independent variables, and only 2% of the variations were not explained by the model. Moreover, all the adjusted R^2 and predicted R^2 were also found to be below ~0.20 from each other, indicating reasonable agreement on how well the models were able to predict a response value. The experimental data obtained were also found to be reliable, based on the high adequate precision values of above 4 that were obtained, as presented in Table 5. The adequate precision measured the signal-to-noise ratio, and the range of predicted values at the design points were then compared to the average prediction error [40].

Table 5
Summary of correlation coefficients (R^2), adjusted R^2, predicted R^2 and adequate precision for the response of succinate rejection (Y_1), SF of succinate/formate (Y_2) and SF of succinate/acetate (Y_3).

Response	Y_1	Y_2	Y_3
R^2	0.98	0.99	0.98
Adjusted R^2	0.96	0.99	0.95
Predicted R^2	0.81	0.97	0.84
Adequate Precision	26.81	50.79	23.21

3.2.1. Analysis of variance (ANOVA)

The analysis of variance (ANOVA) of the developed models was evaluated using several methods, including the F-value, lack-of-fit and p-value. Table 6 presents the F-values obtained from the developed models (Eq. (11)–(13)). The F-values were greater than the critical F-value (3.67 at 95% significance) obtained from the standard distribution table, with degrees of freedom equal to 9 and 7. The large F-values of 50.19, 179.69 and 42.76 for the ANOVA of succinate rejection, SF of succinate/formate and SF of succinate/acetate, respectively confirmed the sufficiency of the developed models. Moreover, the p-values (prob. > F) related to all the models were <0.05, which means that the models were statistically significant at a confidence level of 95%.

Table 6
ANOVA results for succinate rejection and SFs of succinate/formate and succinate/acetate, and estimated regression coefficient.

Source	Degree of Freedom	Succinate Rejection (%)		Succinate/Formate SF		Succinate/Acetate SF	
		F Value	P Value	F Value	P Value	F Value	P Value
Model	9	50.19	<0.0001	179.69	<0.0001	42.76	<0.0001
A	1	139.52	<0.0001	900.8	<0.0001	223.98	<0.0001
B	1	0.13	0.7247	20.22	0.0028	2.9	0.1324
C	1	181.48	<0.0001	292.7	<0.0001	54	0.0002
A^2	1	41.17	0.0004	290.23	<0.0001	70.78	<0.0001
B^2	1	8.39	0.0231	1.01	0.3474	0.37	0.5604
C^2	1	15.81	0.0054	9.65	0.0172	17.64	0.004
AB	1	1.4	0.2757	11.01	0.0128	1.3	0.2915
AC	1	60.33	0.0001	53.69	0.0002	9.25	0.0188
BC	1	5.13	0.0578	40.45	0.0004	7.77	0.027
Residual	7						
Lack of Fit	3	3.39	0.1345	0.67	0.6114	1.4	0.3659
Pure Error	4						

Further justification of the adequacy of the models came from the evaluation using lack-of-fit, which signified the difference between the experimental results and model predictions, except for the random error [42]. From Table 6, the F-values of the lack-of-fit for the quadratic models were also found to be lower than the critical F-value (6.59 at 95% significance), with degrees of freedom equal to 3 and 4. These values signified that the lack-of-fit of the developed models was insignificant and consequently showed that the models were suitable to be used to predict the succinate rejection and SFs within the range of the studied variables.

3.2.2. Pareto analysis

Fig. 5 presents the Pareto graphic analysis for all the developed models. As can be seen from Fig. 5A, among all the terms, the quadratic of the crosslinking time (A^2) followed by the crosslinking time (A) and the succinate concentration in the feed (C) showed the highest influence on the succinate rejection, with $\beta_A^2 = 52.03\%$, $\beta_A = 42.65\%$ and, $\beta_c = 4.24\%$, respectively. Meanwhile, for the SFs of succinate/formate and succinate/acetate, the crosslinking time (A) and quadratic of the crosslinking time (A^2) were shown to have the greatest influence, with $\beta_A = 79.90\%$, $\beta_A^2 = 19.65\%$ and $\beta_A = 90.59\%$, $\beta_A^2 = 9.12\%$, respectively. Overall, this result signified that the most influential term in determining the performance of the PI/GO MMM was the crosslinking time, based on the large percentage of β obtained from all the models. This may have been because the crosslinking time affected both the structure and properties of the membrane, which consequently influenced its overall performance.

3.3. Membrane separation performance

3.3.1. Pure water flux of the membrane

Fig. 6 presents the permeation of the membrane before and after the cross-linking with EDA, which was calculated using Eq. (3). From the figure, the pure water flux of the membrane increased with the cross-linking. This is believed to have been due to the replacement of the imide group in the MMM by the highly hydrophilic amine group from

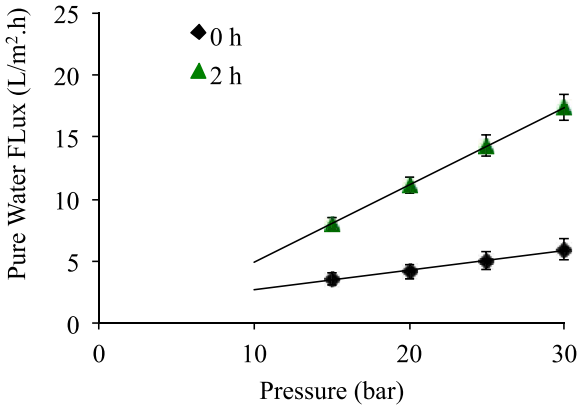

Fig. 6. Pure water flux of MMM before and after 2 h of cross-linking with EDA.

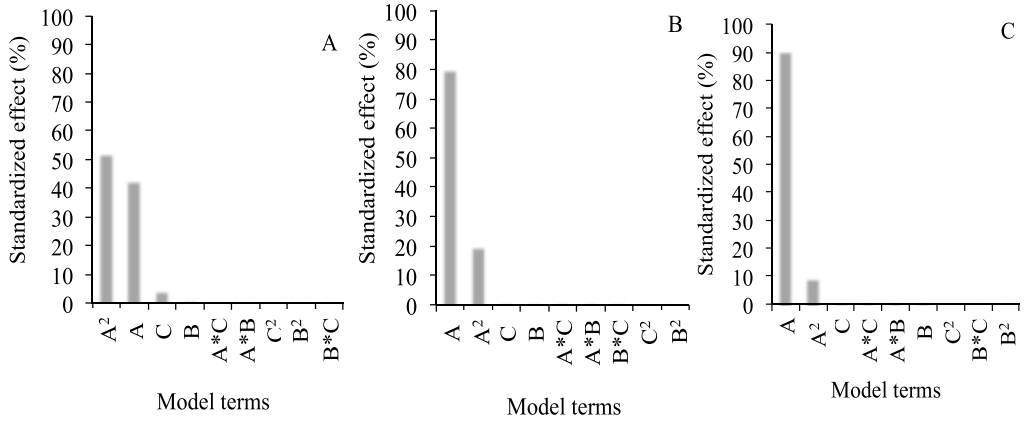

Fig. 5. Pareto graphic analysis of the relative effects of the first order, quadratic, and interaction terms on A) succinate rejection, B) SF of succinate/formate, and C) SF of succinate/acetate.

the EDA, as demonstrated in the FT-IR result (refer to Fig. 2). The result was also supported by the reduced contact angle observed after the cross-linking process (refer to Table 3). However, when compared to the commercial membrane, the permeation of the cross-linked MMM was still considered to be low, and seemed to require further attention. One of the possible reasons for the low flux performance of the MMM would be the physical structure of the PI P84, which possesses a compact chain packing that could have created a high resistance to water permeability [43]. Nevertheless, the addition of the amine cross-linker from the EDA demonstrated an improved and consistent rejection performance, even when the feed concentration was increased to 50 g/L, and it also increased the flux performance, even though it was still not up to par with that of the commercial membrane. A further improvement to the flux may be possible through the use of different types of diamine cross-linkers with different lengths and chemical structures [17].

3.3.2. *Membrane rejection performance: effect of model variables*

In this section, the surface responses regarding succinate rejection and selectivity for each experimental condition are discussed, based on the effects of the interaction of the most influential parameters to the least influential ones, as determined from the Pareto analysis presented in Section 3.2.2. The sequence of the parameters was as follows; crosslinking time, succinate concentration in the feed, and membrane evaporation time. The selectivity of the succinate with respect to the monovalent anions (formate and acetate) was represented by the SF value calculated using Eq. (5). A membrane with a high succinate selectivity will have a low SF value that is close to 0 and vice versa. All the conditions for the experiments and graphs were designed and generated by the RSM.

a) Interaction Effects of the Most Significant Parameter: Crosslinking Time

Interaction effect of crosslinking time and succinate concentration in feed: Fig. 7 demonstrates the interaction effect of the crosslinking time and the succinate concentration in the feed at a constant membrane evaporation time of 45 s. From Fig. 7A, at a feed concentration of 10 g/L, the MMM performed well at 0 h crosslinking time (not crosslinked), and a high succinate rejection of 89% was observed. However, as the succinate concentration in the feed was increased to up to 50 g/L, the rejection performance of the MMM started to deteriorate by 73%, which was the highest reduction in succinate rejection observed in this study. This was indicated by the large drop in the slope of the succinate graph with respect to the succinate concentration in the feed at a crosslinking time of 0 h (refer to Fig. 7A). However, at a crosslinking time of 1 h, the steepness of the slope of the succinate rejection graph started to decrease, representing only a 33% drop with an increasing succinate concentration of up to 50 g/L (refer to Fig. 7A). Interestingly, a further improvement was seen at the extended crosslinking time of 2 h, where only a 7% drop in succinate rejection was seen (refer to Fig. 7A). Utilizing the MMM fabricated at a crosslinking time of 2 h, the membrane rejection was then found to be successfully maintained above a rejection of 80% when the feed concentration was supplied at between 10 and 50 g/L.

The successful improvement in the rejection of succinate using the MMM crosslinked with EDA was also observed in the selectivity performance of the membrane. Fig. 7A (i and ii) shows that for the membrane at a crosslinking time of 0 h, the increase in succinate concentration of up to 50 g/L led to an increase in the SFs at around 47%

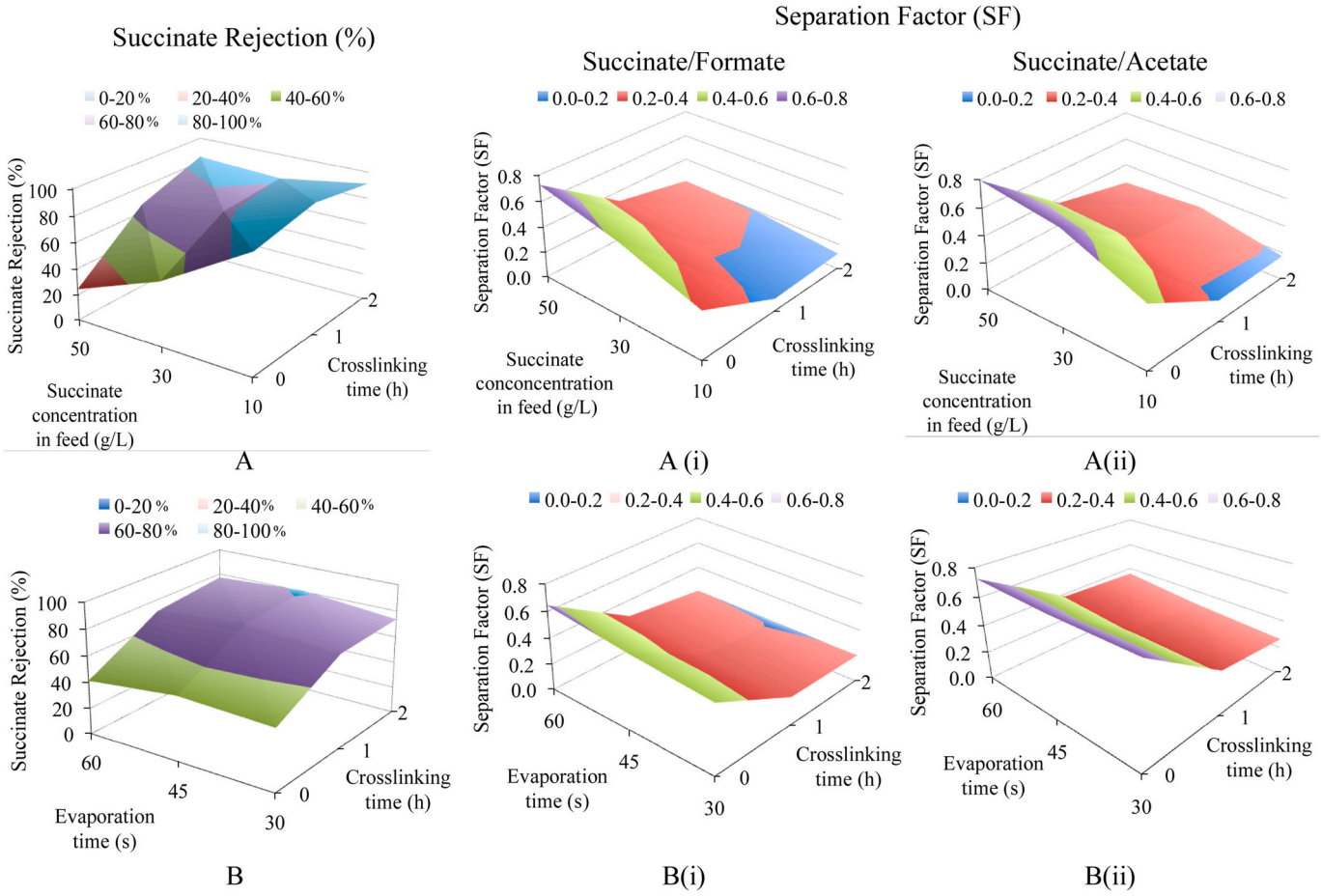

Fig. 7. Interaction effects between A) crosslinking time and succinate concentration in feed, and B) crosslinking time and evaporation time on succinate rejection (%) and separation factor (SF) (Constant parameters utilized; A) 45s evaporation time, B) 30 g/L succinate concentration).

and 41% for the succinate/formate and succinate/acetate ratios, respectively, indicating a reduced selectivity of the membrane towards succinate. However, as the MMM was crosslinked for 2 h, the SFs of the membrane decreased toward 0, as indicated by the reduction in the slope of the graph of the SFs with respect to the crosslinking time, as presented in Fig. 7A (i and ii). This indicated that the selectivity of MMM was improving compared to the non-crosslinked membrane, which agreed with the rejection performance of the crosslinked MMM, as discussed in the previous paragraph.

The phenomenon occurred in the neat PI/GO MMM (0 h crosslinking time), where the performance of the membrane was severely reduced with increasing feed concentration. This could have been due to several reasons, including, but not limited to, the ion-polymeric membrane interactions that influenced the salt diffusion across the membrane. Generally, at low salt concentrations in the feed, such as 10 g/L in this study, strong interactions between the salt and the charged polymeric membrane, such as electrostatic repulsive forces, may act to hinder the diffusion of the salt. Thus, this could have contributed to the high rejection performance of the membrane. However as the salt concentration increased, the ion-polymeric membrane interactions were increasingly screened, raising the salt diffusion coefficient and consequently, reducing the membrane rejection and selectivity performances, which were reflected in the results presented in Fig. 7B [44,45]. Nevertheless, this phenomenon was found to have severely affected the performance results of the non-crosslinked MMM. Even though in a previous study [14], the presence of GO in a PI-based membrane successfully overcame the reduction in the rejection performance of the membrane with increasing concentrations of sodium sulphate in the feed solution, this phenomenon was not observed in this study. Possible reasons for this could be the much higher concentration of the feed that was used in this study, which was up to 50 g/L compared to 21 g/L that was reported in the previous study, and the different feed solution properties that were utilized, where a mixture solution (succinate, formate and acetate) was used in this study compared to the single solute used in the previous one [14].

In contrast, improvements were observed in the membrane rejection (Fig. 7A) and SF (Fig. 7A (i and ii)) performances of the crosslinked MMM with increasing crosslinking time. This could have been due to the changes in the properties of the MMM when the EDA crosslinker was introduced. According to the FT-IR (refer to Fig. 2), the crosslinking with EDA, which introduced covalent bonding between the PI polymer chains and GO, created the effects of networking and hole-filling [46]. Thus, this could have limited the movement of the polymer chains, increased the rigidity of the chain structure, and reduced the interstitial spaces across the membrane [47]. This was also well supported by the XRD analysis (refer to Fig. 4), which demonstrated a reduction in the d-spacing of the MMM with crosslinking time. During the separation of the succinate from the mixture of by-products, the reduced interstitial spaces and restricted movement of the polymeric chains from the crosslinking process created a higher steric resistance for the big molecules and allowed only the small molecules to pass through, unlike the non-crosslinked MMM. Thus, this resulted in an increase in the membrane rejection, as reported in the previous study [39,46]. Moreover, succinate, which is a divalent anion, has a larger size compared to the monovalent anions of both formate and acetate, thus explaining the increased rejection of succinate with an extended crosslinking time. A similar phenomenon was also observed in the study by Kim et al. (2020), which showed that the crosslinking of PI using a diamine crosslinker tightens and causes the polymer chains to be rigid, subsequently enhancing the packing of the chains and reducing the inter-segmental mobility. The changes in the structure of the membrane and the reduction in the d-spacing provided the membrane with a desirable rejection and selectivity [39].

Interaction of crosslinking time and the time for the solvent to evaporate from the membrane phase: Fig. 7B shows the effects of the interaction of the crosslinking time and the time for the solvent to evaporate from the membrane phase on the succinate rejection and SFs at a constant succinate feed concentration (30 g/L). Overall, increasing the solvent evaporation time had only a slight effect on the performance of the membrane. This was indicated by the small peak that was observed at 45 s of evaporation time in Fig. 7B for every crosslinking time that was investigated. The succinate rejection only improved by around 4–8%. In contrast, when the crosslinking times were increased to 1 and 2 h, the membrane rejection performance was significantly increased by 36% and 39.5%, respectively. The highest succinate rejection of 80% was successfully achieved for the membrane that had been prepared at 45 s of evaporation time and 2 h of crosslinking time (refer to Fig. 7B). A similar trend was also observed in Fig. 7B (i and ii) for the SFs of the membrane. There was a greater reduction in the SFs of the membrane with increasing crosslinking time, from 0.58 to 0.19 and from 0.71 to 0.30 for the succinate/formate and succinate/acetate ratios, respectively. The decreasing SFs, which approached 0, indicated an improvement in the selectivity of the succinate over the by-products.

To investigate the influence of the interaction effects of the crosslinking time and evaporation time on the membrane performance, the swelling property of the membrane was investigated. Initially, the membrane was immersed in 30 g/L of succinate solution, and the degree of swelling was determined using Eq. (2). From the results, the degree of swelling of the membrane was found to be inversely proportional to the succinate rejection. The higher the reduction in the degree of swelling, the higher was the succinate rejection. In contrast, at a crosslinking time of 2 h, the swelling of the membrane was found to have been reduced by around 29, 46 and 41% for membrane evaporation times of 30 s, 45 s and 60 s, respectively. The highest reduction in swelling was obtained for the membrane with an evaporation time of 45 s, representing the largest improvement in the succinate rejection (39.5%), as observed in Fig. 7B. The result was also in agreement with the FT-IR and XRD presented in Figs. 1 and 3, which demonstrated the formation of covalent bonds because of the replacement of amide by the amine groups, and the reduction in the MMM d-spacings. This reduction in swelling indicated that the movement of the polymer chains was restricted to accommodate the bigger-sized succinate divalent ions compared to the monovalent formate and acetate ions. As a result, an improved succinate rejection was observed, as can be seen in Fig. 7B [48,49]. Shen et al. (2016) also discussed the phenomenon of a higher divalent anion rejection in comparison to the monovalent anions across the restricted narrow-sized membrane pores, based on the electrostatic interaction of the ion-water molecules. It was easier to remove the hydrogen-bonded water molecules that were attracted to the monovalent anions than the divalent anions, due to their lower charge. Thus, this enabled the monovalent anions to easily penetrate the membrane compared to the divalent anion, succinate [50]. Thus, this explained the increase in the succinate rejection that was observed in this work in investigating the increase in the rigidity of the membrane at a crosslinking time of 2 h.

b) Interaction Effects of the Least Significant Parameter: Time for Solvent to Evaporate from the Membrane Phase

Interaction of time for solvent to evaporate from the membrane phase and the succinate concentration in the feed: Fig. 8 shows the surface response and contour plot of the interaction effects of the membrane evaporation time and concentration of succinate in the feed for the 1-h crosslinked MMM. Similar to Fig. 4B, it was shown that the evaporation time had a very minimal effect on the performance of the membrane. Fig. 8 demonstrates a plateau in the performance of the succinate rejection with increasing evaporation time at any feed concentration that was investigated, except for the most concentrated succinate feed solution of 50 g/L. In this condition, the membrane that was fabricated at 30 s of evaporation time (shortest) exhibited a succinate rejection of only 57%, the lowest rejection achieved in this study (green zone in Fig. 8A). Overall, from Fig. 8, the crosslinking time of 1 h was seen to have been insufficient to sustain the succinate rejection

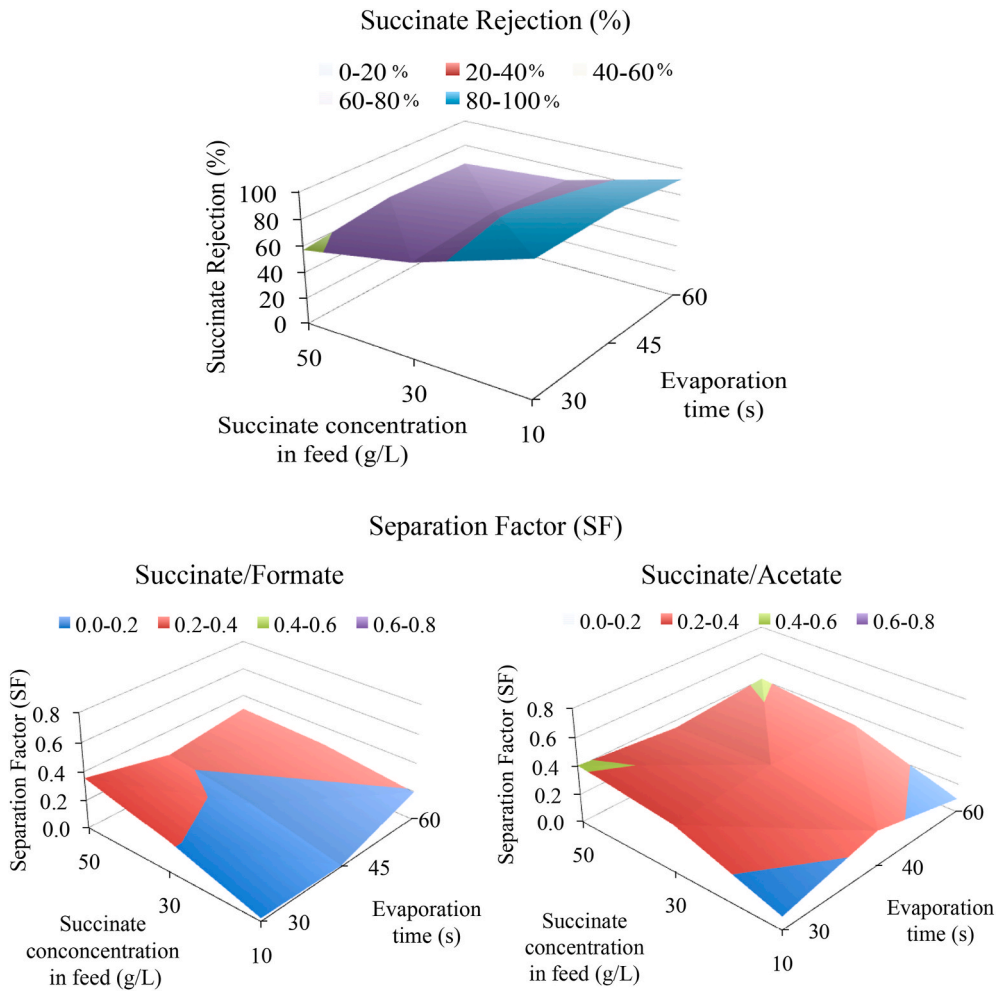

Fig. 8. Interaction effects between the least significant parameters; time for the solvent to evaporate from the membrane phase and the succinate concentration in the feed on the succinate rejection (%) and separation factor (SF) (Constant parameters utilized; crosslinking time of 1 h).

performance above 80%, as observed in Fig. 8A. As the concentration of the succinate was increased from 10 to 50 g/L, it was observed that there was a 30–40% reduction in the succinate rejection, depending on the membrane evaporation time. A similar trend was also observed for the membrane selectivity, as presented in Fig. 8C (i and ii). As was previously discussed in Section 3.3.2, this phenomenon may have been due to the insufficient crosslinking of the membrane. At increasing feed concentrations, the solution entering the membrane could have moved the polymer chain apart and increased the overall volume of the membrane. Thus, apart from the monovalent ions (formate and acetate), the bigger divalent ions (succinate) could also pass through the membrane [51]. Thus, this phenomenon could have disrupted the crystalline property of the membrane to some extent.

From the evaluation of the effects of the model variables, the interaction effects between the crosslinking time and the succinate concentration in the feed exhibited the most dominant effects on the performance of the membrane compared to the other combined variables. This result supported the statistical analysis obtained from the Pareto study in Section 3.2.2, which found that the crosslinking time was the most influential parameter, followed by the succinate concentration in the feed, and the solvent evaporation time.

Overall the identification of the critical fabrication conditions that influences membrane properties via optimization is believed could minimize the future workload for optimization stage. Apart from the influence of the input parameters investigated on the membrane properties and its consequent membrane performance discussed in this work, the relationship between them have also been intensively discussed in the previous studies. For instance, membrane contact angle was seen influenced by the changes in the membrane polymer concentration. In the study by Haddadpour et al. (2018) [52], the increase in polymer concentration has increased the membrane contact angle and reduced the pore size. The increased in the polymer concentration has led to the formation of thin dense layer (the thin dense layer of membrane become thicker) on the membrane surface [52], which in the study resulted in the increased in membrane's rejection performance, but reduced membrane permeability. It is also important to note that every membrane property can be influenced by more than one fabrication parameters, which is consistent with the results obtained from Ref. [52]. They observed that, apart from the polymer concentration, the membrane pore size was also influenced by the solvent evaporation time. The increase in membrane evaporation time was seen increases the thickness of the membrane top layer, consequently reduces the membrane pore size affecting the membrane performances [52]. In other study reported by Ref. [53], the membrane properties such as Zeta potential was found could also be tailored accordingly by membrane modification using compounds with known charged such as PSS (polystyrene sulfonic acid) and TEPA (tetraethylpentamine). The modification of PVDF with TEPA resulted in highly positively charged membrane with +23 mV Zeta potential due to the presence of large amount of protonated amino functions on the membrane surface. Meanwhile for the modification of PVDF with PSS, the membrane becomes highly negatively charged of −54 mV [53]. The membrane Zeta potential indication helps to understand the

effect of membrane fouling and permeation flux [53]. Thus from numerous studies that have reported on the membrane properties characterized by various means, optimization of the input parameters is deemed as crucial in determining the membrane properties that could influence membrane performances.

3.4. Optimization and model validation

For the optimization and model validation, the input variables were set at a crosslinking time of between 1 and 2 h, minimum evaporation time of 30s and succinate concentration of between 30 and 50 g/L. The input variables were set based on the interaction effects of the variables on the observed responses. For the responses, the succinate rejection was designed to achieve the maximum values, whereas the SF of the succinate with respect to the formate and acetate were set at a minimum value of 0 to achieve a high selectivity of succinate. Using these conditions, three (3) replicate experiments were carried out to validate the accuracy of the predicted model. The predicted optimal input conditions were found to be at a crosslinking time of 1.61 h, evaporation time of 30 s, and succinate concentration of 30 g/L with a good desirability of D = 0.81.

Table 7 presents the predicted responses and the experimental runs that were determined from the predicted optimal input conditions provided by the RSM together with the succinate recovery and degree of removal of by-products calculated using Eq. (4) and Eq. (5), respectively. From the table, the confirmatory experiments showed that the succinate rejection and SF of the succinate with respect to formate and acetate were obtained at the respective values of 81%, 0.18 and 0.26, which were close to the predicted results of 75%, 0.17 and 0.25, respectively. At optimal conditions, the complete removal of acetate with a negative rejection was achieved, similar to the previously reported studies utilizing the commercial membranes NF270, NF-DK and NF-DL [8,54]. The negative rejection was due to the preferential solvation of the formate ions, which had a lower charge and size compared to succinate. Generally, a negative rejection occurs when at least two ions of similar charge with different sizes and/or charge numbers are present in the feed solution. The large size and/or higher-charged ion will be strongly expelled from the membrane surface, giving rise to a pull-in of the small and/or low-charged ions of the same charge into the pores of the membrane. The increase in the ion concentration in the membrane phase resulted in a negative rejection [55]. This phenomenon was also occasionally observed in previous studies [56–58]. However, for the acetate, the remaining concentration was still present, and could be further removed with a series of separation processes (refer to Table 7). The higher removal of formate compared to acetate was probably due to the higher dissociation constant of formic acid (K_a 1.77 $\times$ 10^{-5}) compared to acetic acid (K_a 1.76 $\times$ 10^{-4}), indicating that formate could be more readily dissociated [59]. Thus, a higher removal of formate was observed compared to acetate.

The estimated errors between the predicted and experimental values of the succinate rejection and SFs of succinate/acetate and succinate/formate were calculated using Eq. (8) and were recorded at 6.7%, 4.0% and 3.8%, respectively. The small percentage errors of less than 10% confirmed the adequacy of the selected model and the evaluated properties, and further approved the validity of the obtained model to produce the targeted membrane with the desired responses. The deviation between the predicted and experimental (±10%) values could be attributed to a combination of both measurement and experimental errors.

3.4.1. Performance of the crosslinked MMM

The optimal conditions achieved from the RSM were also investigated using an actual fermentation broth with a similar succinate concentration of 30 g/L as the model solution, and by-product concentrations of 4.9 g/L of acetate and 8.0 g/L of formate. Overall, the diafiltration process of the actual fermentation broth recorded a volume concentration factor (VCF) of around 1.7, with an average final flux that was higher than 12.3 L/m^2.h.

The summary of the rejection performance of the optimized EDA-crosslinked PI/GO MMM using the diafiltration process is also presented in Table 8. From the table, the diafiltration process increased the recovery of succinate after every cycle, where the succinate was successfully recovered within the range of 69.8–86%. When compared to the model solution, even at the first stage of the diafiltration process using the optimized crosslinked MMM, the result of the succinate recovery from the actual fermentation broth at 69.8% was within 10% of the percentage error. Thus, this confirmed the adequacy of the model, even when an actual fermentation broth was utilized.

Apart from the increased succinate recovery, the diafiltration process also demonstrated an increase in the removal of the formate and acetate of up to 57.3% and 92%, representing the SF values of 0.33 and 0.15, respectively. This indicated that the selectivity of succinate was also enhanced. Moreover, the crosslinked MMM also demonstrated a 96% FRR with irreversible fouling of 4%, which indicated a low fouling property, as presented in Fig. 9. Equations (9) and (10) were used to calculate the membrane fouling property.

The successful application of the optimized EDA-crosslinked PI/GO MMM for succinate recovery and selectivity from an actual fermentation broth indicated the significance of the optimization process that was carried out. The performance of the optimized EDA-crosslinked MMM was found to be comparable to commercial membranes, even at a high feed concentration and/or high concentrations of by-products (refer to Table 9). It can be concluded that the optimization assisted in understanding the complex separation process in the recovery of succinate using the crosslinked MMM, and subsequently, in overcoming the trade-off limitation between the performance of the membrane and the increasing succinate concentration in the feed. The RSM application was also found to be a more economical approach in extracting the maximum amount of information at a minimum number of experiments with promising results.

4. Conclusions

PI/GO MMM crosslinked with EDA was successfully fabricated via both the phase inversion immersion precipitation technique and chemical POST crosslinking using EDA. This crosslinked MMM was characterized, and the performance was verified using a concentrated succinate feed solution, where the membrane demonstrated a substantial improvement in its rejection performance. The crosslinking process successfully reduced the drop in the rejection of succinate when the

Table 7
Succinate recovery and removal of by-products for the predicted model and experimental runs using optimal conditions obtained from RSM.

Membrane	Model Solution							
	Succinate		Formate			Acetate		
	Initial conc. (30 g/L)		Initial conc. (15 g/L)			Initial conc. (15 g/L)		
	Final conc. (g/L)	Rejection (%)	Final conc. (g/L)	Removal (%)	SF	Final conc. (g/L)	Removal (%)	SF
Predicted Response	22.7	75.8	<0	100.0	0.17	0.48	96.8	0.25
Experimental Run	24.3	81.0	<0	100.0	0.18	4.05	73.0	0.26

Table 8
Succinate rejection and removal of by-products (formate and acetate) using diafiltration experiment.

Dia-filration stages	Actual Fermentation Broth							
	Flux (L/m^2.h)		Succinate		Acetate		Formate	
	Initial	Final	Final conc. (g/L)	Rejection (%)	Final conc. (g/L)	Removal (%)	Final conc. (g/L)	Removal (%)
1st stage	17.8	12.3	20.9	69.8	4.2	85.2	3.34	42.0
2nd stage	17.7	14.6	23.0	74.1	3.1	78.4	2.26	49.4
3rd stage	19.8	14.6	26.6	86.0	2.2	92.0	1.42	57.3

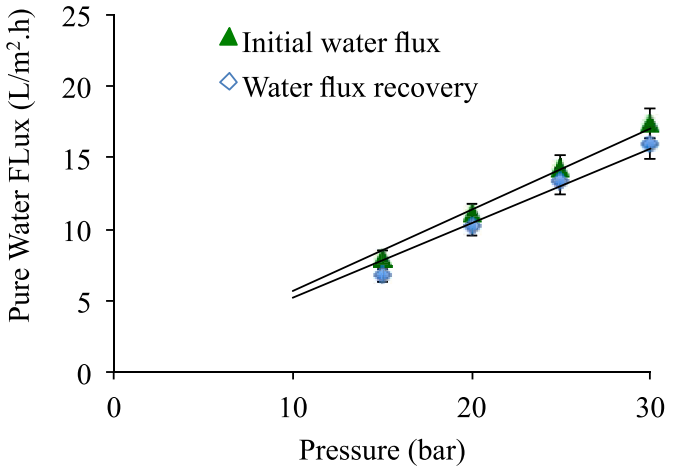

Fig. 9. Pure water flux of the membrane before and after the recovery of succinate from the fermentation broth.

concentration of succinate rose to 50 g/L. A reduction of 73% in the rejection of succinate for the neat MMM was successfully lowered to 33%, and subsequently to 7% when the membrane was crosslinked at 1 and 2 h, respectively. A significant improvement was also seen in the selectivity of the membrane from the reduced SF values that approached 0. The formation of covalent bonds between the PI chains and the reduced d-spacing were found to be responsible for the improved performance of the MMM. It was also seen that the optimized MMM was not only applicable for the model solution, but also for an actual fermentation broth. With the actual broth, a succinate recovery of 86%, SF of 0.15-0.33, and flux recovery ratio of 96% were achieved.

The diafiltration that was carried out using the actual fermentation broth also demonstrated a comparable rejection performance of succinate and selectivity with the model solution and commercial NF membranes, even when a concentrated feed was utilized. A statistical analysis using a Box-Behnken design that was carried out in this study also validated the significance of the selected input parameters on the performance of the fabricated membrane. The experimental results obtained showed that there was good agreement with the predicted R^2 value of 0.98 obtained from the ANOVA analysis. From the statistical analysis, the most significant factors affecting the performance of the membrane were also indicated as follows: 1) the crosslinking time, 2) succinate concentration in the feed, and 3) the time for the solvent to evaporate from the membrane phase. The optimized study with a desirability function of 0.81 provided information on the interactions and influence of parameters on achieving a membrane with a high rejection and selectivity, especially in a concentrated succinate feed solution. The RSM application thus ensured a sustainable and more economical approach in minimizing the number of experiments, the time consumed and the use of chemicals for the fabrication of an effective membrane.

Table 9
Rejection of succinate and by-products for commercial NF membranes and EDA-crosslinked PI/GO MMM.

NF membrane	Fermentation composition	Concentration of feed	Salt Rejections	References
EDA-crosslinked MMM membrane	Mixture of succinate, formate and acetate	30 g/L succinate 4.9 g/L acetate 8 g/L formate	Suc = 86% Ace = 8% For = 42.7%	This study
Commercial NF45	Mixture of succinate, formate, acetate and lactate	48.6 g/L succinate 6.8 g/L formate 8.2 g/L acetate 11.2 g/L lactate	Suc = 78.2% For = -97.6% Ace = −54.6% Lac = −18.3%	[54]
Commercial composite polyamide (ES10 and NF270)	Single solute solutions of succinic, formic, acetic, propionic and citric acids	0.500 g/L	ES10: Suc = 80–99% NF270: Suc = 90–100%	[9]
Commercial NF270, NF-DK and NF-DL	Mixture solution of succinate, formate, acetate	10.00 g/L succinate 7.14 g/L formate 6.66 g/L acetate	NF-DK: Suc = 86.6% For ≈ −25.0%, Ace ≈ 35.0% NF270: Suc = 88.9% For ≈ −15.0% Ace ≈ 37.0% NF-DL: Suc = 79.0% For ≈ −25.0% Ace ≈ −10.0%	[8]

Funding

This work was supported by the Ministry of Higher Education Malaysia (MOHE) under the Fundamental Research Grant Scheme [FRGS/1/2018/TK02/UKM/02/2]; Universiti Kebangsaan Malaysia (UKM) under Dana Impak Perdana [DIP/2019/12].

Author statement

Nadiah Khairul Zaman: Conceptualization, Methodology, Investigation, Formal analysis, Data curation, Writing – original draft preparation, Rosiah Rohani: Validation, Fund acquisition, Writing – review and editing. Izzati Izni Yusoff: Software, Data curation, Abdul Wahab Mohammad: Fund Acquisition, Abdullah Amru Indera Luthfi: Resources, Investigation, Suriani Abu Bakar: Resources.

Declaration of competing interest

The authors declare that they have no known competing financial interests or personal relationships that could have appeared to influence the work reported in this paper.

Acknowledgement

The authors would like to express their gratitude to the Ministry of Science, Technology and Innovation, Malaysia (MOSTI) and Universiti Kebangsaan Malaysia (UKM) for the funding. Also, the authors wish to thank UKM for the postdoctoral researcher scheme under Dana Modal Insan.

References

[1] J.P. Tan, J.M. Jahim, T.Y. Wu, S. Harun, T. Mumtaz, The effects of reducing power from metal carbonate on succinic acid production using Actinobacillus succinogenes, Jurnal Kejuruteraan 79 (5–3) (2017), https://doi.org/10.11113/jt.v79.11328.

[2] J.J. Bozell, G.R. Petersen, Technology development for the production of biobased products from biorefinery carbohydrates—the us department of energy's "top 10" revisited, Green Chem. 12 (2015) 539, https://doi.org/10.1039/B922014C.

[3] C.D.N. Newswire, Bio Succinic Acid Market 2020 : CAGR of 25.9% with Top Countries Data, Latest Trends, Market Size, Share, Global Industry Analysis & Forecast To 2026, MarketWatch, 2020.

[4] P.I. Omwene, M. Yagcioglu, Z.B.O. Sarihan, A. Karagunduz, B. Keskinler, Recovery of succinic acid from whey fermentation broth by reactive extraction coupled with multistage processes, J. Environ. Chem. Eng. 8 (2020), 104216, https://doi.org/10.1016/j.jece.2020.104216.

[5] P.-C. Chang, H.-Y. Hsu, G.-W. Jang, Biological routes to itaconic and succinic acid, Phy. Sci. Rev. 1 (2016), https://doi.org/10.1515/psr-2016-0052.

[6] H.B. Park, J. Kamcev, L.M. Robeson, M. Elimelech, B.D. Freeman, Maximizing the right stuff: the trade off between membrane permeability and selectivity, Science 356 (2017) eaab0530, https://doi.org/10.1126/science.aab0530.

[7] N.K. Zaman, R. Rohani, A.W. Mohammad, A.M. Isloor, J.M. Jahim, Investigation of succinic acid recovery from aqueous solution and fermentation broth using polyimide nanofiltration membrane, J. Environ. Chem. Eng. 8 (2020), 101895, https://doi.org/10.1016/j.jece.2017.09.047.

[8] P.A. Sosa, C. Roca, S. Velizarov, Membrane assisted recovery and purification of bio-based succinic acid for improved process sustainability, J. Membr. Sci. 501 (2016) 236–247, https://doi.org/10.1016/j.memsci.2015.12.018.

[9] J.-H. Choi, K. Fukushi, K. Yamamoto, A study on the removal of organic acids from wastewaters using nanofiltration membranes, Separ. Purif. Technol. 59 (2008) 17–25, https://doi.org/10.1016/j.seppur.2007.05.021.

[10] C.C.J. Leung, A.S.Y. Cheung, A.Y.-Z. Zhang, K.F. Lam, C.S.K. Lin, Utilization of waste bread for fermentative succinic acid production, Biochem. Eng. J. 65 (2012) 10–15, https://doi.org/10.1016/j.bej.2012.03.010.

[11] P. Khunnonkwao, K. Jantama, S. Kanchanatawee, S. Galier, H.R. Balmann, A two steps membrane process for the recovery of succinic acid from fermentation broth, Separ. Purif. Technol. 207 (2018) 451–460, https://doi.org/10.1016/j.seppur.2018.06.056.

[12] G. Bargeman, J.M. Vollenbroek, J. Straatsma, C.G.P.H. Schroen, R.M. Boom, Nanofiltration of multi-component feeds. Interactions between neutral and charged components and their effects on retention, J. Membr. Sci. 247 (2005) 11–20, https://doi.org/10.1016/j.memsci.2004.05.022.

[13] M. Manttari, M. Nystrom, Critical flux in NF of high molar mass polysaccharides and effluents from the paper industry, J. Membr. Sci. 170 (2000) 257–273, https://doi.org/10.1016/S0376-7388(99)00373-7.

[14] N.K. Zaman, R. Rohani, A.W. Mohammad, A.M. Isloor, Polyimide-graphene oxide nanofiltration membrane: characterizations and application in enhanced high concentration salt removal, Chem. Eng. Sci. 177 (2018) 218–233, https://doi.org/10.1016/j.ces.2017.11.034.

[15] X.L. Wang, C.H. Zhang, P. Quyang, The possibility of separating saccharides from a NaCl solution by using nanofiltration in diafiltration mode, J. Membr. Sci. 204 (2002) 271–281, https://doi.org/10.1016/S0376-7388(02)00050-9.

[16] J. Luo, Y. Wan, Effect of highly concentrated salt on retention of organic solutes by nanofiltration polymeric membranes, J. Membr. Sci. 372 (2011) 145–153, https://doi.org/10.1016/j.memsci.2011.01.066.

[17] K. Vanherck, A. Cano-Odena, G. Koeckelberghs, T. Dedroog, I.F.J. Vankelecom, A simplified diamine crosslinking method for PI nanofiltration membranes, J. Membr. Sci. 353 (2010) 135–143, https://doi.org/10.1016/j.memsci.2010.02.046.

[18] D. Saeki, M. Imanishi, Y. Ohmukai, T. Maruyama, H. Matsuyama, Stabilization of layer-by-layer assembled nanofiltration membranes by crosslinking via amide bond formation and siloxane bond formation, J. Membr. Sci. 447 (2013) 128–133, https://doi.org/10.1016/j.memsci.2013.07.022.

[19] J. Xu, L. Xu, H. Xu, F. Sun, X. Gao, C. Gao, Stability and permeation behavior of a porous membrane modified by polyelectrolyte networks enabled by electro-deposition and cross-linking for water purification, J. Membr. Sci. 496 (2015) 21–30, https://doi.org/10.1016/j.memsci.2015.08.053.

[20] A. Bos, H. Punt, M. Strathmann, M. Wessling, Suppression of gas separation membrane plasticization by homogeneous polymer blending, AIChE J. 47 (2001) 1088–1093, https://doi.org/10.1002/aic.690470515.

[21] C. Liu, L. Shi, R. Wang, Crosslinked layer-by-layer polyelectrolyte nanofiltration hollow fiber membrane for low-pressure water softening with the presence of SO42− in feed water, J. Membr. Sci. 486 (2015) 169–176, https://doi.org/10.1016/j.memsci.2015.03.050.

[22] Y. Zheng, G. Yao, Q. Cheng, S. Yu, M. Liu, C. Gao, Positively charged thin-film composite hollow fiber nanofiltration membrane for the removal of cationic dyes through submerged filtration, Desalination 328 (2013) 42–50, https://doi.org/10.1016/J.DESAL.2013.08.009.

[23] C. Qiu, S. Qi, C.Y. Tang, Synthesis of high flux forward osmosis membranes by chemically crosslinked layer-by-layer polyelectrolytes, J. Membr. Sci. 381 (2011) 74–80, https://doi.org/10.1016/j.memsci.2011.07.013.

[24] J.P. Tan, J.M. Jahim, S. Harun, T.Y. Wu, T. Mumtaz, Utilization of oil palm fronds as a sustainable carbon source in biorefineries, Int. J. Hydrogen Energy (2015) 1–11, https://doi.org/10.1016/j.ijhydene.2015.08.034.

[25] A.A.I. Luthfi, J.M. Jahim, S. Harun, J.P. Tan, A.W. Mohammad, Biorefinery approach towards greener succinic acid production fromoil palm frond, https://doi.org/10.1016/j.ijhydene.2015.08.034 bagasse, Process Biochem. 51 (2016) 1527–1537, https://doi.org/10.1016/j.procbio.2016.08.011.

[26] N.K. Zaman, R. Rohani, A.W. Mohammad, Fabrication of highly selective amine-cross-linked membrane for concentrated bio-succinate recovery from both synthetic model solutions and fermentation broth, J. Water Process Eng. 37 (2020), 101420, https://doi.org/10.1016/j.jwpe.2020.101420.

[27] K. Vanherck, G. Koeckelberghs, I.F.J. Vankelecom, Crosslinking polyimides for membrane applications: a review, Prog. Polym. Sci. 38 (2013) 874–896, https://doi.org/10.1016/j.progpolymsci.2012.11.001.

[28] Z. Lazic, Design of Experiments in Chemical Engineering, WILEY-VCH Verlag GmbH & Co. KGaA., Weinheim, 2004.

[29] H. Koolivand, A. Sharif, M.R. Kashani, M. Karimi, M.K. Salooki, M.A. Semsarzadeh, Functionalized graphene oxide/polyimide nanocomposites as highly CO2-selective membranes, J. Polym. Res. 21 (2014) 599, https://doi.org/10.1007/s10965-014-0599-9.

[30] W. Choi, J. Choi, J. Bang, J.-H. Lee, Layer-by-Layer assembly of graphene oxide nanosheets on polyamide membranes for durable reverse-osmosis applications, American Chem. Soc. 5 (2013) 12510–12519, https://doi.org/10.1021/am403790s.

[31] A. Georgiev, D. Dimov, E. Spassova, J. Assa, P. Dineff, G. Danev, Chemical and physical properties of polyimides: biomedical and engineering applications, in: M. J.M. Abadie (Ed.), High Performance Polymers - Polyimides Based - from Chemistry to Applications, InTech 2012.

[32] F. Samadaei, M. Salami-Kalajahi, H. Roghani-Mamaqani, M. Banaei, A structural study on ethylenediamine-and poly(amidoamine)-functionalized graphene oxide: simultaneous reduction, functionalization and formation of 3D structure, RSC Adv. 5 (2015) 71835–71843, https://doi.org/10.1039/c5ra12086a.

[33] I.W. Mwangi, J.C. Ngila, Removal of heavy metals from contaminated water using ethylenediamine-modified green seaweed (Caulerpa serrulata), Phys. Chem. Earth 50–52 (2012) 111–120, https://doi.org/10.1016/j.pce.2012.08.015.

[34] Y. Zhuang, X. Liu, Y. Gu, Molecular packing and properties of poly(benzoxazole-benzimidazole-imide) copolymers, Polym. Chem. 3 (2012) 1517, https://doi.org/10.1039/C2PY20074K.

[35] B.-S. Ge, T. Wang, H.-X. Sun, W. Gao, H.-R. Zhao, Preparation of mixed matrix membranes based on polyimide and aminated graphene oxide for CO2 separation, Polym. Adv. Technol. 29 (2017) 1334–1343, https://doi.org/10.1002/pat.4245.

[36] B. Feng, K. Xu, A. Huang, Synthesis of graphene oxide/polyimide mixed matrix membranes for desalination, RSC Adv. 7 (2017) 2211, https://doi.org/10.1039/c6ra24974d.

[37] W.-S. Hung, C.-H. Tsou, M.D. Guzman, Q.-F. An, Y.-L. Liu, Y.-M. Zhang, C.-C. Hu, K.-R. Lee, J.-Y. Lai, Cross-linking with diamine monomers to prepare composite graphene oxide-framework membranes with varying d-spacing, Chem. Mater. 26 (2014) 2983–2990, https://doi.org/10.1021/cm5007873.

[38] W. Qiu, C.-C. Chen, L. Xu, L. Cui, D.R. Paul, W.J. Koros, Sub-Tg cross-cinking of a polyimide membrane for enhanced CO2 plasticization resistance for natural gas separation, Macromolecules 44 (2011) 6046–6056, https://doi.org/10.1021/ma201033j.

[39] S.-J. Kim, Y. Ahn, J.-F. Kim, S.-E. Nam, H. Park, Y.H. Cho, K.-Y. Baek, Y.-I. Park, Comparison of liquid-phase and methanol-swelling crosslinking processes of polyimide dense membrane for CO2/CH4 separation, J. Appl. Polym. Sci. (2020), e49860, https://doi.org/10.1002/app.49860.

[40] M. Mourabet, A.E. Rhilassi, H.E. Boujaady, M. Bennani-Ziatni, A. Taitai, Use of response surface methodology for optimization of fluoride adsorption in an aqueous solution by Brushite, Arabian J. Chem. 10 (2014) S3292–S3302, https://doi.org/10.1016/j.arabjc.2013.12.028.

[41] A. Das, S. Mishra, Removal of Textile dye Reactive Green-19 using bacterial Consortium: process optimization using response surface methodology and kinetics study, J. Environ. Chem. Eng. 5 (2017) 612–627, https://doi.org/10.1016/j.jece.2016.10.005.

[42] V. Vatanpour, M. Sheydaei, M. Esmaeili, Box-Behnken design as a systematic approach to inspect correlation between synthesis conditions and desalination performance of TFC RO membranes, Desalination 420 (2017) 1–11, https://doi.org/10.1016/j.desal.2017.06.022.

[43] X. Qiao, T.-S. Chung, K.P. Pramoda, Fabrication and characterization of BTDA-TDI/MDI (P84) co-polyimide membranes for the pervaporation dehydration of isopropanol, J. Membr. Sci. 264 (2005) 176–189, https://doi.org/10.1016/j.memsci.2005.04.034.

[44] G.M. Geise, D.R. Paul, B.D. Freeman, Fundamental water and salt transport properties of polymeric materials, Prog. Polym. Sci. 39 (2014) 1–42, https://doi.org/10.1016/j.progpolymsci.2013.07.001.
[45] R.J. Klein, D.T. Welna, A.L. Weikel, H.R. Allcock, J. Runt, Counter-ion effects on ion mobility and mobile ion concentration of doped polyphosphazene and polyphosphazene ionomers, Macromolecules 40 (2007), 5-3990, https://doi.org/10.1021/ma070357o.
[46] X.Y. Qiao, T.S. Chung, Diamine modification of P84 polyimide membranes for pervaporation dehydration of isopropanol, AIChE J. 52 (2006) 3462–3472, https://doi.org/10.1002/aic.10964.
[47] G.M. Geise, H.B. Park, A.C. Sagle, B.D. Freeman, J.E. McGrath, Water permeability and water/salt selectivity tradeoff in polymers for desalination, J. Membr. Sci. 369 (2011) 130–138, https://doi.org/10.1016/j.memsci.2010.11.054.
[48] V.S. Praptowidodo, Influence of swelling on water transport through PVA-based membrane, J. Mol. Struct. 739 (2005) 207–212, https://doi.org/10.1016/j.molstruc.2004.04.035.
[49] G.M. Geise, C.L. Willis, C.M. Doherty, A.J. Hill, T.J. Bastow, J. Ford, K.I. Winey, B. D. Freeman, D.R. Paul, Characterization of aluminum-neutralized sulfonated styrenic pentablock copolymer films, Ind. Eng. Chem. Res. 52 (2013) 68–1056, https://doi.org/10.1021/ie202546z.
[50] M. Shen, S. Keten, R.M. Lueptow, Dynamics of water and solute transport in polymeric reverse osmosis membranes via molecular dynamics simulations, J. Membr. Sci. 506 (2016) 95–108, https://doi.org/10.1016/j.memsci.2016.01.051.
[51] R.M. Hodge, G.H. Edward, G.P. Simon, A.J. Hill, Water absorption and states of water in semicrystalline poly(vinyl alcohol) films, Polymer 37 (1996) 6–1371, https://doi.org/10.1016/0032-3861(96)81134-7.
[52] N. Haddadpour, Z. Ahmadi, Z. Shariatinia, F. Afshari Taromi, Nanofiltration membranes based on PA6/EVOH with variable composition and morphology, J. Vinyl Addit. Technol. 25 (2018), https://doi.org/10.1002/vnl.21613.
[53] D. Breite, M. Went, A. Prager, A. Schulze, The critical zeta potential of polymer membranes: how electrolytes impact membrane foulding, RSC Adv. 6 (2016) 98180–98189, https://doi.org/10.1039/C6RA19239D.
[54] S.H. Kang, Y.K. Chang, Removal of organic acid salts from simulated fermentation broth containing succinate by nanofiltration, J. Membr. Sci. 246 (2005) 49–57, https://doi.org/10.1016/j.memsci.2004.08.014.
[55] A.E. Yaroshchuk, Negative rejection of ions in pressure-driven membrane processes, Adv. Colloid Interface Sci. 139 (2008) 150–173, https://doi.org/10.1016/j.cis.2008.01.004.
[56] I. Koyuncu, D. Topacik, M.R. Wiesner, Factors influencing flux decline during nanofiltration of solution containing dyes and salts, Water Res. 38 (2004) 432–440, https://doi.org/10.1016/j.watres.2003.10.001.
[57] A. Perez-Gonzalez, R. Ibanez, P. Gomez, A.M. Urtiaga, I. Ortiz, J.A. Irabien, Nanofiltration separation of polyvalent and monovalent anions in desalination brines, J. Membr. Sci. 473 (2015) 16–27, https://doi.org/10.1016/j.memsci.2014.08.045.
[58] H.K. Londsdale, W. Pusch, A. Walch, Donnan-membrane effects in hyperfiltration of ternary systems, J. Chem. Soc. Faraday Trans. 1 (71) (1975) 501–504, https://doi.org/10.1039/F19757100501.
[59] K. Staszak, M.J. Wozniak, Z. Karas, J. Staniewski, K. Prochaska, Application of nanofiltration in the process of the separation of model fermentation broth components, Pol. J. Chem. Technol. 15 (4) (2013) 1–4, https://doi.org/10.2478/pjct-2013-0058.